# Performance comparison of compact heat exchangers suitable for chloride Molten Salt Fast Reactor intermediate heat transport system

Sunghyun Yoo [a], In Woo Son [a], Sungwook Choi [a], Jeong Ik Lee[a*]
[a]*Dept. Nuclear & Quantum Eng., KAIST, 373-1, Guseong-dong, Yuseong-gu, Daejeon, 305-701, Republic of Korea*
[*]*Corresponding author: jeongiklee@kaist.ac.kr*

## 1. Introduction

The Molten Salt Reactor (MSR) is one of the Gen-IV reactors that has many potential advantages over conventional nuclear reactors, such as high thermal efficiency, improved safety, and high compactness. The Molten Salt Fast Reactor (MSFR) is one of MSRs which utilizes a fast neutron spectrum. However, the system design is mostly based on the experience of graphite-moderated molten salt breeder reactor at Oak Ridge National Laboratory (ORNL) in the 1960s. According to the Gen-IV International Forum (GIF), an MSFR is being actively studied by many research institutes among GIF member states [1].

As mentioned earlier, an MSFR has many advantages over conventional reactors. This reactor type is economical because the core can operate above 600°C, resulting in high thermal efficiency. An MSFR also has improved safety because the core is at low pressure and there is no risk of meltdown accidents because the nuclear fuel and coolant are already in the form of liquid [2]. An MSFR has the advantage of reducing high level radioactive waste by incinerating the actinides produced by conventional nuclear power plants.

In an MSFR, chloride salts with low neutron absorption are preferred over fluoride salts. A chloride salt has lower melting point (450°C or less) than that of a fluoride salt, which widens the operating range of the reactor. Stainless steel can be used as a structural material instead of a Ni-based alloy. Additionally, a chloride salt has lower viscosity than a fluoride salt and requires smaller pumping power [3].

In the previous studies, a Plate Fin Heat Exchanger (PFHE) based primary Intermediate Heat eXchanger (IHX) suitable for an MSFR was designed [4, 5]. However, in this study, in addition to PFHE, a Printed Circuit Heat Exchanger (PCHE) and a Plate Heat Exchanger (PHE) are designed to compare their performances to those of PFHE. The most suitable primary IHX type for chloride MSFR can be determined from the study. NaCl-$MgCl_2$ was selected as the chloride salt for the MSFR based on the operating temperature range of the reactor and the thermal properties of the molten salt.

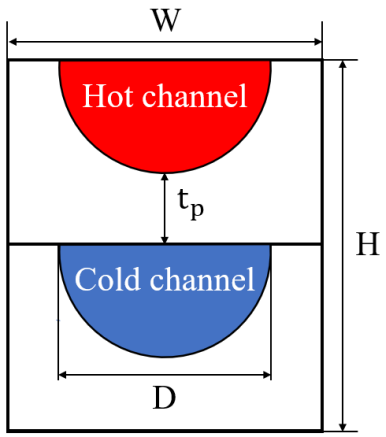


Fig. 1. The basic geometry of PCHE

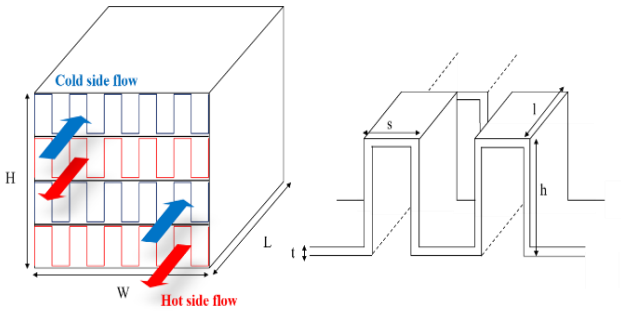


Fig. 2. The structure of offset-strip fin type PFHE

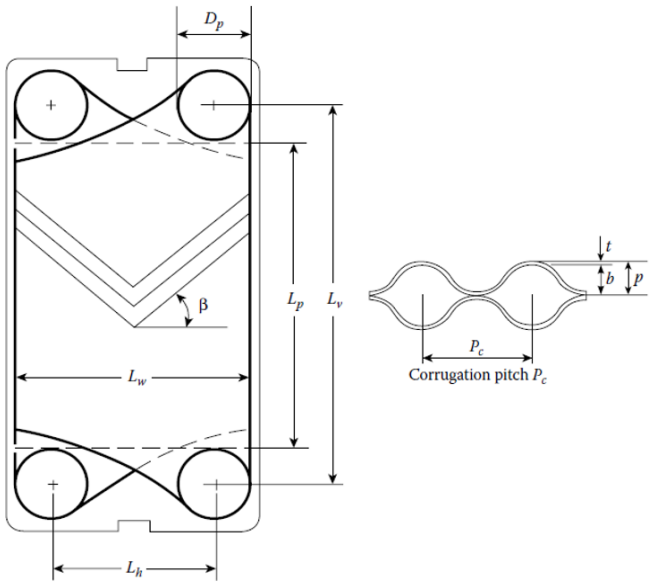


Fig. 3. The main dimensions of PHE [10]

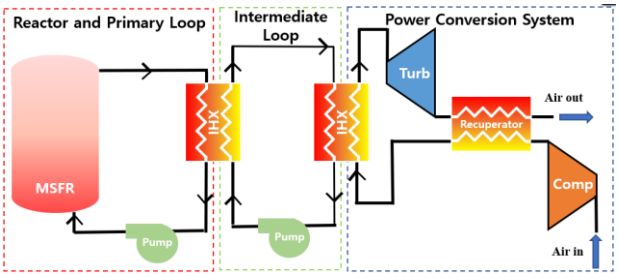


Fig. 4. The layout of the MSFR system

## 2. Methodology

As in the previous studies, the power conversion system of the chloride MSFR was initially optimized using the KAIST-OCD (Open Cycle Design), an in-house code [4, 5]. The algorithm of the KAIST-OCD code for the cycle optimization is shown in Fig 5. The open Brayton cycle optimization parameters and results are summarized in Tables 1 and 2. The core outlet temperature of chloride MSFR was fixed at 650°C and this condition was established by referring to the MSRE report from ORNL [7].

The reactor core thermal output is assumed to be 0.2 $MW_{th}$. This is because compact heat exchangers including PFHE are currently commercialized in the scale of 0.2 $MW_{th}$.

Table 1. Cycle optimization parameters

| Fixed variable | |
|---|---|
| Air intake Temperature / Humidity | 15 °C / Dry |
| Max Temperature | 650 °C |
| Thermal heat | 0.2 $MW_{th}$ |
| Compressor inlet Pressure | 101.325 kPa |
| Turbine efficiency | 88% |
| Compressor efficiency | 84% |
| Recuperator effectiveness | 0.90 |

Table 2. Cycle optimization results

| | |
|---|---|
| Cycle thermal efficiency (%) | 31.05 |
| Cycle net work ($MW_e$) | 0.06 |
| Specific work (MWe/kg) | 0.0695 |
| Thermal heat ($MW_{th}$) | 0.2 |
| Pressure ratio | 2.55 |
| Max. Pressure (MPa) | 0.288 |
| Mass flow rate (kg/s) | 0.8635 |

The thermal sizing of the chloride MSFR system is performed with cycle optimization. In this process, the mass flowrate of primary IHX was calculated to simultaneously satisfy 10K pinch temperature and the maximum temperature of NaCl-$MgCl_2$ in the heat exchanger. The thermal properties of molten salt are shown in Table 4 [8].

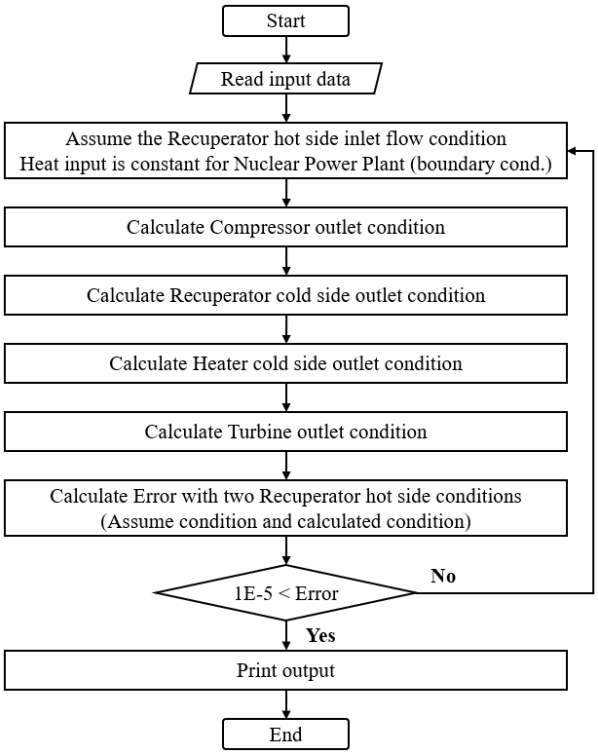


Fig. 5. Algorithms of KAIST-OCD [4, 5]

Table 3. MSR Primary PFHE thermal sizing results for the MSR system [6, 7]

| Heat load | 0.2 $MW_{th}$ |
|---|---|
| $\Delta T_{hot\ side\ inlet-cold\ side\ outlet}$ | 10 K [6] |
| Primary PFHE hot side [7] | |
| Mass flow rate (kg/s) | 5.535 |
| Inlet temperature (°C) | 650 |
| Outlet temperature (°C) | 600 |
| Primary PFHE cold side | |
| Mass flow rate (kg/s) | 3.578 |
| Inlet temperature (°C) | 590 |
| Outlet temperature (°C) | 640 |

Table 4. Thermal properties of the NaCl-$MgCl_2$ [8]

| |
|---|
| $C_P = 1080.19\ [J/kg \cdot K]$ |
| $\rho = (2518 - 0.406 \times T), for\ T < 973K$<br>$\rho = (2297.1 - 0.507 \times T), for\ T > 973K [kg/m^3]$ |
| $\mu = \left(0.000286 \times exp\left(\frac{1441}{T}\right)\right)\ [kg/m \cdot s]$ |
| $k = 0.3133 + 0.000267 \times T\ [W/m \cdot K]$ |

Finally, PCHE, PFHE, and PHE for primary IHX were designed for the chloride MSFR system. The channel of the PCHE was selected to have a zigzag shape, and the PFHE was selected as an offset-strip fin type, which has a higher convective heat transfer coefficient compared to other fin types. PHEs are categorized according to the corrugation shape of a plate, and in this study, the

commonly used chevron type plate was assumed for the design.

The first step for designing the primary IHX is to optimize the geometry parameters of each HX to maximize heat exchange effectiveness and minimize volume. The geometry parameters of each heat exchanger are shown in Figs. 1-3, and the range of design parameters is shown in Tables 5-7. The structural material for all primary IHXs was chosen to be SS316 (SA-213 TP316H), which can withstand temperatures as high as 800 °C.

Table 5. Primary PCHE design parameters range

| | Min. | Max. |
|---|---|---|
| Flow length (m) | 0.75 | 1.5 |
| Hot, Cold diameter [D] (mm) | 1.55 | 2 |
| Mesh number | 200 | |
| Plate material | SS316L | |
| Plate thickness (mm) | 1 | |

Table 6. Primary PFHE design parameters range [4, 5]

| | Min. | Max. |
|---|---|---|
| Hot flow length (m) | 0.3 | 2 |
| Hot, Cold Fin height [H] (mm) | 0.2 | 9 |
| Fin thickness [t] (mm) | 0.1 | 0.2 |
| Hot, Cold Fin frequency [1/n] (mm) | 0.4 | 1.4 |
| Fin offset length [l] (mm) | 1 | 10 |
| Number of hot side layers | 40 | 60 |
| Plate material | SS316L | |
| Plate thickness (mm) | 0.5 | |

Table 7. Primary PHE design parameters range [10, 13]

| | Min. | Max. |
|---|---|---|
| Projected plate length [$L_p$] (m) | 0.1 | 0.7 |
| Plate width length [$L_w$] (m) | 0.1 | 0.3 |
| Channel gap [$b$] (mm) | 2 | 5 |
| Port diameter [$D_p$] (mm) | 5 | |
| Chevron angle [$\beta$] (°) | 30 | 60 |
| Total number of plates | 50 | 200 |
| Plate material | SS316L | |
| Plate thickness (mm) | 0.5 | |

Since a detailed description of the design process and geometry of the PCHE and PFHE can be found in the previous works [5, 9], PHE design method will be only discussed in this study. The following correlations for the Nusselt number *Nu* and the Fanning friction factor *j* are used [10]:

$$Nu = C_h Re^n Pr^{0.33} \left(\frac{\mu_b}{\mu_w}\right)^{0.17} \quad (1)$$

$$f = \frac{K_p}{Re^{0.3}} \quad (2)$$

The constants used in formulas (1) and (2) can be found in the reference [10]. The pressure drop can be obtained from equation (3) [10]:

$$\Delta p_c = 4f \frac{L_{eff} N_p}{D_h} \frac{G_c^2}{2\rho} \left(\frac{\mu_b}{\mu_w}\right)^{-0.17} \quad (3)$$

where $\Delta p_c$ is the channel pressure drop, $L_{eff}$ is the effective flow length between the inlet and outlet ports, $N_p$ is the number of passes, $D_h$ is the hydraulic diameter, $G_c$ is the channel mass flux, $\rho$ is the density of the fluid flowing inside the channel. $\mu_b/\mu_w$ is the ratio of the dynamic viscosity at bulk mean temperature and wall temperature, and since the hydraulic diameter of PHE is very small, it can be assumed that $\mu_b/\mu_w \approx 1$. Equation (4) is used for the form loss calculation for PHE:

$$\Delta p_p = 1.4 N_p \frac{G_p^2}{2\rho} \quad (4)$$

where $\Delta p_p$ is the port pressure drop, $G_p$ is the port mass flux.

## 3. Results and Discussions

The results of the conceptual design of primary IHXs for the Chloride MSFR are summarized in Table 8. The PHE had the lowest pressure drop and surface area density. The PFHE had the highest pressure drop, but the PFHE had the smallest heat exchanger volume and the largest surface area density of the three heat exchanger types. It is noted that the surface area density is the total heat transfer area divided by the volume core.

Table 8. Comparison of MSR primary IHX design

| | PCHE | PHE | PFHE |
|---|---|---|---|
| Hot side pressure drop [kPa] | 11.53 | 5.44 | 15.76 |
| Cold side pressure drop [kPa] | 6.98 | 3.01 | 9.05 |
| HX width [m] | 0.225 | 0.20 | 0.15 |
| HX length [m] | 0.225 | 0.50 | 0.513 |
| HX height [m] | 1.0 | 0.27 | 0.20 |
| Volume core [$m^3$] | 0.0506 | 0.027 | 0.0150 |
| Hot side heat transfer area [$m^2$] | 26.22 | 6.45 | 13.59 |
| Cold side heat transfer area [$m^2$] | 26.22 | 6.45 | 13.83 |
| Surface area density [$m^2/m^3$] | 1036.36 | 477.78 | 1828 |

Since the PCHE is designed assuming it has a zigzag channel, the heat transfer performance is higher than that of the straight channel type PCHE, but the pressure loss due to friction becomes larger. PFHE also has a very

small hydraulic diameter and a complex flow path structure, so the heat transfer area is very large, but the pressure loss due to friction is also the largest of the three heat exchanger types [11, 12].

The heat transfer performance of PHE is determined by the chevron angle, $\beta$. The higher the value of $\beta$, the higher the *Nu* is, but the corresponding pressure drop penalty is also significantly higher [10]. According to the reference, the friction factor of PHE is up to 10-400 times higher than that of conventional shell-and-tube type heat exchangers [13]. Despite the high friction coefficient of PHE, the actual pressure drop is not large. This is because the nominal velocity of the fluid in a channel is low, so the resulting pressure drop is much smaller than that of other types of heat exchanger. In addition, the amount of flow required to achieve the target NTU value is less than that of other heat exchangers, so the pressure loss due to form loss is minimized, resulting in high heat transfer performance with small pressure drop [13].

## 4. Conclusions and Further Works

In this study, PCHE, PFHE, and PHE were designed as primary IHXs for chloride-based MSFR and their performances were compared. The three heat exchangers are representative types of compact heat exchangers, which are compact in size (high heat transfer area/volume ratio) but high heat transfer performance compared to conventional shell and tube type heat exchangers.

The conceptual design results showed that the PFHE had the highest pressure drop, but the smallest overall heat exchanger volume and the highest surface area density. PHE had the lowest surface area density but also had the lowest pressure loss of the three heat exchanger types. This result can be explained by the structural characteristics of each heat exchanger.

The complex flow path configuration of the PFHE ensures good heat transfer performance, but results in very large pressure drops due to friction.

In the case of PHE, the friction factor of the plates is high, but the nominal velocity of the fluid in the channel of PHE is low, so the actual pressure loss is small. Furthermore, since a PHE requires fewer flow paths than other heat exchanger types to reach the target NTU value, the form loss is minimized, allowing good heat transfer performance with low pressure loss.

Since many studies on PHE using molten salt as a fluid have not yet been performed, the feasibility of PHE designed in this study will be verified using CFD (Computational Fluid Dynamics) methods in further study.

## ACKNOWLEDGEMENTS

This work was supported by Korea Research Institute for defense Technology planning and advancement (KRIT) grant funded by the Korea government (DAPA(Defense Acquisition Program Administration)) (21-107-F00-018(KRIT-CT-22-017), Next Generation Multi-Purpose High Power Generation Technology (Development of Power Generating System Core-Technologies for Liquid Fuel Heat Generator), 2022)

## REFERENCES

[1] Generation IV International Forum 2016 Annual Report, 2016.
[2] Dolan, T. J. (n.d.). Molten salt reactors and thorium energy. Elsevier.
[3] Holcomb, D. E., Flanagan, G. F., Patton, B. W., Gehin, J. C., Howard, R. L., & Harrison, T. J. (2011). Fast spectrum molten salt reactor options. ORNL/TM-2011/105.
[4] Yoo, S., Son, I. W., Choi, S., & Lee, J. I. Primary PFHE design for chloride based molten salt fast reactor. Transactions of Korean Nuclear Society Autumn Meeting (2022)
[5] Son, I. W., Choi, S., Kim, S. J., & Lee, J. I. Heat exchanger design study for micro molten salt reactor. Transactions of Korean Nuclear Society Spring Meeting (2022)
[6] Son, I. W., Choi, S., Kim, S. J., & Lee, J. I. Thermal-sizing of the molten salt reactor system with gas Brayton cycle. Transactions of Korean Nuclear Society Virtual Autumn Meeting (2021)
[7] Robertson, R. C. "MSRE design and operations report part I: description of reactor design." ORNL-TM-728, Oak Ridge National Laboratory (1965).
[8] Williams, D. F. Assessment of candidate molten salt coolants for the NGNP/NHI heat-transfer loop. No. ORNL/TM-2006/69. Oak Ridge National Lab. (ORNL), Oak Ridge, TN (United States), 2006.
[9] Baik, S. J., Kim, S. G., Son, S. M., & Lee, J. I. (2015, September). Printed circuit heat exchanger design, analysis and experiment. In NURETH-16 (2015). ANS.
[10] Kakaç Sadik, Liu, H., & Pramuanjaroenkij, A. (2012). Heat exchangers: Selection, Rating, and Thermal Design, third edition. CRC Press.
[11] Kwon, J. S., Son, S., Heo, J. Y., & Lee, J. I. (2020). Compact heat exchangers for supercritical CO2 power cycle application. Energy Conversion and Management, 209, 112666.
[12] Li, Q., Flamant, G., Yuan, X., Neveu, P., & Luo, L. (2011). Compact heat exchangers: A review and future applications for a new generation of high temperature solar receivers. Renewable and Sustainable Energy Reviews, 15(9), 4855-4875.
[13] Thulukkanam, K. (2017). Heat Exchanger Design Handbook. CRC press.